1

BIOLOGICAL APPLICATIONS OF MULTIFUNCTIONAL MAGNETIC NANOWIRES

Edward J. Felton and Daniel H. Reich

1.1 INTRODUCTION

Nanoscale magnetic particles are playing an increasingly important role as tools in biotechnology and medicine, as well as for studying biological systems. With appropriate surface functionalization, they enable the selective application of magnetic forces to a wide range of cells, subcellular structures, and biomolecules, and have been applied to or are being developed for areas including magnetic separation, magnetic biosensing and bioassays, drug delivery and therapeutics, and probes of the mechanical and rheological properties of cells [1–10]. Despite these successes, however, the structure of the magnetic particles in common use limits the range of potential applications. Most biomagnetic particles available today are spherical, with either (a) a "core-shell" structure of concentric magnetic and nonmagnetic layers or (b) magnetic nanoparticles randomly embedded in a nonmagnetic matrix [2, 11]. These geometries constrain the range of magnetic properties that can be engineered into these particles, as well as their chemical interactions with their surroundings, because such particles typically carry only a single surface functionality. A new and more versatile approach is to use asymmetric, multisegment magnetic nanoparticles, such as the metal nanowires shown in Figure 1.1.

Biomedical Applications of Nanotechnology. Edited by Vinod Labhasetwar and Diandra L. Leslie-Pelecky

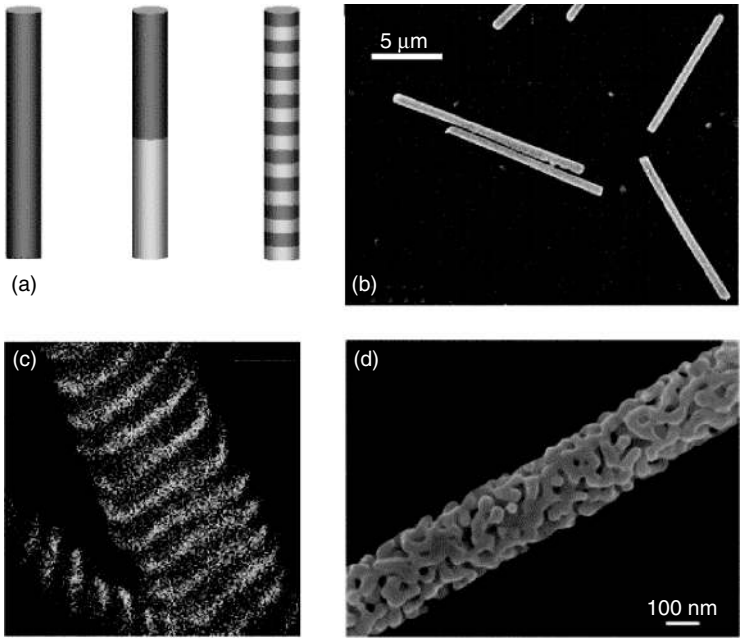

Figure 1.1. (a) Schematic illustration of magnetic nanowires, showing single-segment, two-segment, and two-component multisegment nanowires. (b) SEM image of 15 μm Ni nanowires (from Ref. 24, reproduced with permission of The Royal Society of Chemistry). (c) EELS image of Ni–Cu multisegment nanowires (reprinted with permission from Ref. 15, Copyright 2003, American Institute of Physics). (d) Nanoporous Au–Ag nanowire with Ag etched away. (Reprinted with permission from Ref. 16. Copyright 2003 American Chemical Society.)

The multisegment architecture of these particles, along with the ability to vary the aspect ratio and juxtaposition of dissimilar segments, allows the nanowires to be given a wide range of magnetic, optical, and other physical properties. In addition, differences in the surface chemistry between segments can be exploited to selectively bind different ligands to those segments, enabling the development of magnetic nanoparticle carriers with spatially resolved biochemical functionality that can be programmed to carry out multiple tasks in an intracellular environment.

This chapter provides an overview of recent results of a research program, centered at Johns Hopkins University, that is aimed at development of multifunctional magnetic nanowires for biotechnology applications. Section 1.2 provides a brief introduction to the fabrication process, and this is followed in Section 1.3 by an overview of the physical properties of the nanowires that are important in a biotechnological context. Sections 1.4–1.6 describe our development of the needed "tool-kit" for biological applications: manipulation of the nanowires in suspension, chemical functionalization, and self-assembly techniques. Section 1.7 discusses prospects for magnetic biosensing using nanowires, and Sections 1.8 and 1.9 discuss the major biological applications of

the nanowires explored to date: novel approaches to magnetic separations, new tools for cell positioning and patterning, and new carrier particles for drug and gene delivery.

1.2 NANOWIRE FABRICATION

Nanowires are fabricated by electrochemical deposition in nanoporous templates. Originally developed for fundamental studies of the electrical and magnetic properties of modulated nanostructures [12], this method offers control of both nanowire size and composition and thus allows the nanowires' magnetic and chemical properties to be tailored for specific biological applications. To make the nanowires, a copper or gold conductive film is sputtered on one side of the template to create the working electrode of a three-electrode electrodeposition cell. Metal is then deposited from solution into the template's pores to form the wires. The nanowires' diameter is determined by the template pore size and can range from 10 nm to approximately 1 μm. The wires' length is controlled by monitoring the total charge transferred and is only limited by the thickness of the template. After the nanowire growth is complete, the working electrode film is etched away and the template is dissolved, releasing the nanowires into suspension.

Ferromagnetic nickel nanowires were commonly used in the work reported here. Grown in commercially available 50 μm-thick alumina templates, they have a radius of 175 ± 20 nm and lengths ranging from 5 to 35 μm. An SEM image of 15 μm-long nickel nanowires is seen in Figure 1.1b. The high pore density of the alumina templates (3×10^8 cm^{-2} [13]) enables fabrication of large numbers of nanowires. In addition to single-component nanowires such as these, nanowires comprised of multiple segments can be made by changing the deposition solution during growth. This technique has been used with alumina templates to create two-segment Ni–Au nanowires [14]. Alternatively, multisegment nanowires of certain materials can be grown from a single solution by varying the deposition potential. One example is the alternating ferromagnetic and nonmagnetic layers of the Ni–Cu nanowire shown in Figure 1.1c [15]. Nanowires incorporating two metals can also be synthesized as alloys. In one example, this technique has been used to produce high-surface area nanoporous Au wires by selectively etching away the Ag from Au–Ag alloy nanowires, as shown in Figure 1.1d [16].

1.3 PHYSICAL PROPERTIES

The elongated architecture of the nanowires and the flexibility of the fabrication method permit the introduction of various magnetic and other physical properties. The magnetic properties can be tuned and controlled through the size, shape, and composition of magnetic segments within the wires. For example, due to their high magnetic shape anisotropy, single-segment magnetic nanowires form nearly single-domain states with large remanent magnetizations for a wide range of nanowire lengths. This is illustrated in Figure 1.2, which shows magnetic hysteresis curves for 175 nm-radius nickel nanowires of different lengths [17]. The shape of the hysteresis curves is

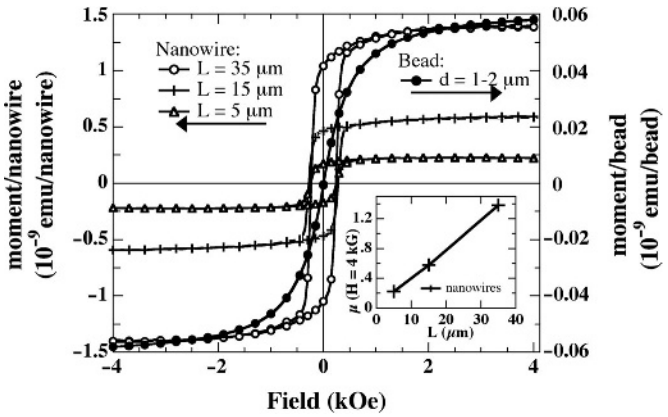

Figure 1.2. Room temperature magnetization versus field curves for 1 to 2 μm beads, 5, 15, and 35 μm nanowires. Inset: Saturation moment versus nanowire size. (Reprinted with permission from Ref. 17. © 2004 IEEE.)

nearly independent of nanowire length, with coercive field $H_C \sim 250$ Oe and remanent magnetization $M_R \sim 0.8M_S$, where M_S is the saturation magnetization. These large, stable, and well-aligned moments make such nanowires useful for low-field manipulations of cells and biomolecules, as discussed in Section 1.8. As seen in the inset, M_S scales linearly with the wire length, and at high fields the nanowires have moment per unit length $\mu/L = 3.9 \times 10^{-11}$ emu/μm. For comparison, Figure 1.2 also shows the magnetic moment of commercially available 1.5 μm-diameter magnetic beads. Note that while the volume of the longest nanowires shown here is only 1.5 times that of the beads, their high-field moment is 20 times that of the beads. Thus the nanowires can provide significantly larger forces per particle in magnetic separations and other high-field applications.

There are, of course, biomagnetic applications in which large magnetic moments in low field are not desirable. These include situations in which it is important to control interactions among particles to reduce agglomeration in suspension. The remanent magnetization of multisegment nanowires such as those shown in Figure 1.1c can be tuned by controlling the shape of the magnetic segments [15, 18, 19]. If the magnetic segments within a multisegment nanowire have an aspect ratio greater than unity, shape anisotropy favors the adoption of a high-remanence state with the segments' moments parallel to the wire axis, even if they are short compared to the length of the nanowire, as shown in Figure 1.3a. In contrast, if the magnetic segments are disk-shaped (aspect ratio < 1), the shape anisotropy of the individual segments favors alignment of their moments perpendicular to the nanowire axis. Dipolar interactions between the segments then favor antiparallel alignment of the moments of neighboring segments, leading to a low-moment state in zero field, as shown in Figure 1.3b.

In addition to defining the magnetic properties, the segment composition can be exploited for other purposes. For example, the high-surface-area nanoporous gold segments previously mentioned (Figure 1.1d) can be used for efficient chemical functionalization, or for biosensing applications. Optical properties of the nanowires can also

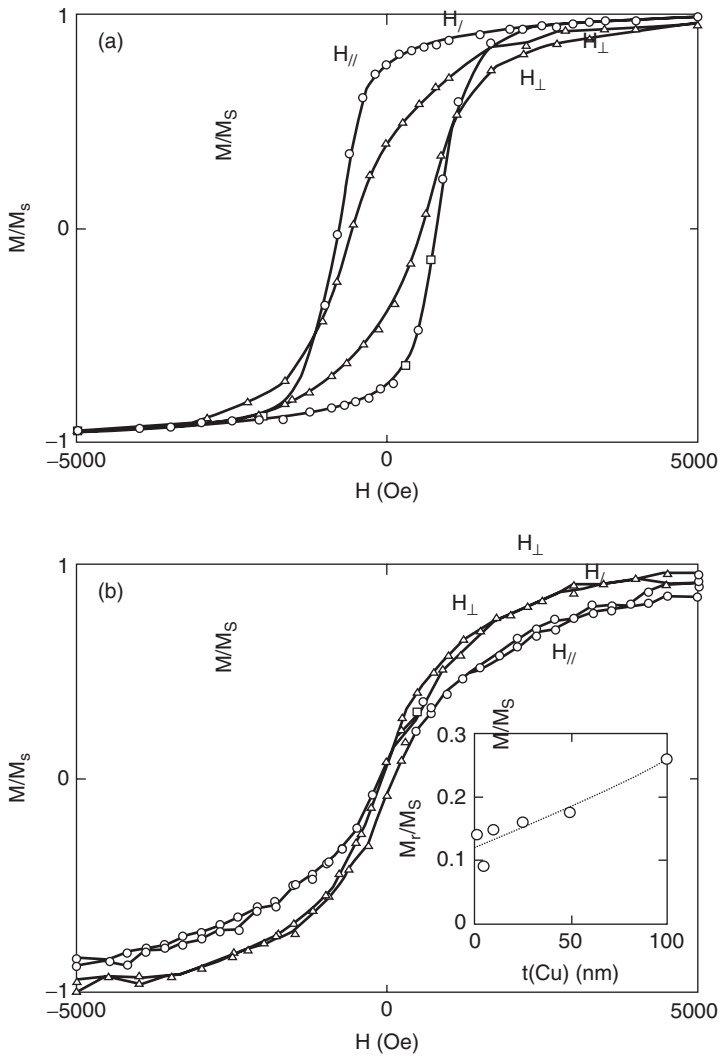

Figure 1.3. Room temperature magnetization versus field curves for arrays of Ni–Cu multilayer nanowires in the template. (a) Ni–Cu nanowires with rod-shaped Ni segments (aspect ratio 2.5) and easy axis parallel to the nanowire axis. (b) Ni–Cu nanowires with disk-shaped Ni segments (aspect ratio 0.1) and easy axis perpendicular to the nanowire axis. The inset shows the remanence for Ni–Cu nanowires with disk-shaped Ni segments as a function of Cu layer thickness. (Reprinted with permission from Ref. 15. Copyright 2003, American Institute of Physics.)

be controlled. Differences in reflectivity in Au–Ag multisegment nanowires are being exploited for "nano-barcoding" of molecules and subcellular structures [20], and oxide segments with intrinsic fluorescence can also be introduced.

1.4 MAGNETIC MANIPULATION OF NANOWIRES

The large and tunable magnetic moments of nanowires allow precise manipulation of molecules and bound cells, with applications ranging from cell separations to two-dimensional cell positioning for diagnostics and biosensing, and to the potential creation of three-dimensional cellular constructs for tissue engineering. The approaches we have developed for these applications take advantage of nanowire–nanowire interactions, as well as their interactions with lithographically patterned micromagnet arrays and external fields. To illustrate these capabilities, we first discuss manipulation of the nanowires themselves.

In liquid suspensions, the nanowires readily orient with their magnetic moments parallel to an applied field. Single-segment and multisegment nanowires with long magnetic segments align with the wire axis parallel to the field, and multisegment wires with disk-shaped segments align perpendicular to the field [15, 21]. When magnetized, the nanowires interact through dipole–dipole magnetic forces. Self-assembly of the nanowires can be achieved, either in suspension or by allowing the wires to settle on flat substrates. This process can be controlled by an external field. Without an applied field, the nanowires are randomly oriented in the suspension, and they will assemble into random collections due to the anisotropy of the dipolar interaction. Application of a small field suppresses this random aggregation by prealigning the nanowires parallel to each other. The nanowires then form end-to-end chains as they settle out of solution, as shown in Figure 1.4 [22]. The addition of descending nanowires to chains settled on the substrate can yield chains that extend over hundreds of micrometers.

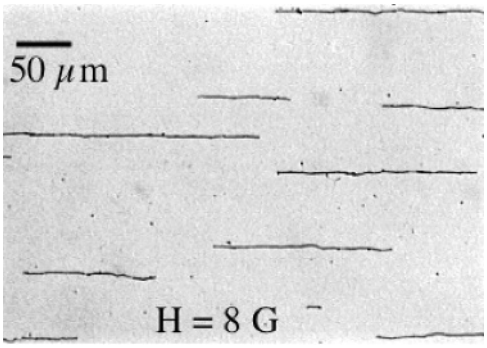

Figure 1.4. Optical micrograph of Ni nanowire chain formation after precipitation from a water suspension in an 8-G external magnetic field. (Reprinted with permission from Ref. 22. Copyright 2002, American Institute of Physics.)

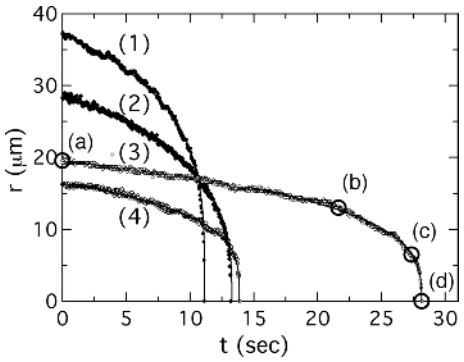

Figure 1.5. Separation versus time for four chain-formation events in a 4-Oe external field. Events (1) and (2) were in water, and events (3) and (4) were in ethylene glycol. (Reprinted from *J Magn Mater*, 249, C. L. Chien et al., Electrodeposited magnetic nanowires: Arrays, field-induced assembly, and surface functionalization, 146–155. Copyright 2002, with permission from Elsevier.)

The motion of both bare nanowires and nanowires bound to cells in suspension is governed by low Reynolds number hydrodynamics, and a nanowire's velocity is given by $\mathbf{v} = \mathbf{F}/D$, where $\mathbf{F}$ is the net force due to external fields, neighboring nanowires, and gravity, and D is the appropriate viscous drag coefficient. Integrating this equation of motion allows precise prediction and modeling of the nanowires' dynamics [21, 23]. For example, Figure 1.5 shows an analysis of a video microscopy study of nanowire chaining dynamics. For all the events shown in Figure 1.5 the wires or chains are nearly collinear. In this case, the force between two wires or chains of lengths L_1 and L_2 is

$$f(r) = -Q_m^2 \left(\frac{1}{r^2} - \frac{1}{(r + L_1)^2} - \frac{1}{(r + L_2)^2} + \frac{1}{(r + L_1 + L_2)^2} \right),$$

where r is the end-to-end separation. The nanowires are described very accurately in this and in all subsequent modeling discussed below as extended dipoles with magnetic charges $\pm Q_m = \pm M \pi a^2$ separated by L, where M is the wire's magnetization. The solid curves are fits to $r(t)$ based on the (somewhat involved) analytic form determined from the one-dimensional equation of motion $dr/dt = \tilde{D} f(r)$, where $\tilde{D} = D_1 D_2/(D_1 + D_2)$ is the reduced drag coefficient. Full details are given in Ref. 21. These results demonstrate that quantitative predictions of the nanowire–nanowire interactions and dynamics can be made.

Another important manipulation tool involves using the strong local fields generated by micrometer-size magnetic features patterned by microlithography on substrates to capture and position nanowires and cells [22, 24, 25]. This "magnetic trapping" process works because the nanowires are drawn into regions of strong local field gradients produced by the patterned micromagnets, such as those at the ends of the Ni ellipses shown in Figure 1.6. The snapshots show video frames from a trapping event, and

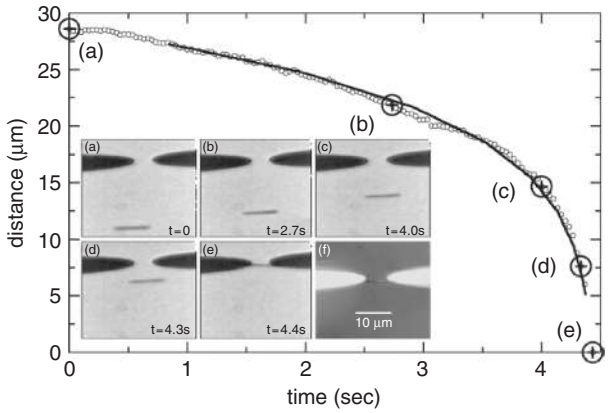

Figure 1.6. Distance from the center of a 10 μm Ni nanowire to the center of the gap between two elliptical micromagnets versus time. A 10 G external magnetic field is oriented parallel to the long axis of the micromagnets. Points (a)–(e) correspond to the inset videomicroscopy images. Inset image (f) is a reflected light image taken after the solvent dried. (Reprinted with permission from Ref. 24. Copyright 2003, American Institute of Physics.)

the trace shows the distance $z(t)$ of the wire from the trap versus time. Analysis of the force produced on the wire by the micromagnets again yields a simple model that can be integrated to obtain $z(t)$ (solid curve). A SEM image of a nanowire trapped by micromagnets is presented in Figure 1.7.

1.5 CHEMICAL FUNCTIONALIZATION

The ability to chemically functionalize nanowires enhances their utility in biological applications. Selectively binding ligands to the surface of nanowires allows additional control of interactions between nanowires, between nanowires and surfaces, and between cells and nanowires, as well as control of the wires' optical characteristics.

We have built on prior knowledge of surface chemistry on planar metallic films [26–28] to selectively functionalize both single- and multicomponent nanowires. Functionalization of nickel utilizes binding between carboxylic acids and metal oxides, in

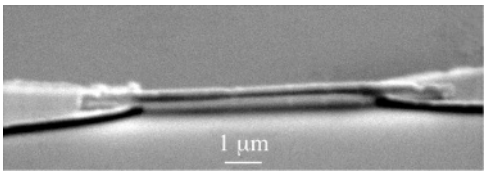

Figure 1.7. SEM image of a nanowire magnetically trapped between two micromanets. (Reprinted with permission from Ref. 22. Copyright 2002, American Institute of Physics.)

this case the native oxide layer present on the nanowires' surface [29], while gold functionalization makes use of the well-known selective binding of thiols to gold [30]. It is therefore possible to attach various molecules possessing a compatible binding ligand to a particular metallic surface. This has been demonstrated with single-segment nickel nanowires that have been functionalized with hematoporphyrin IX dihydrochloride (HemIX), a fluorescent molecule with two carboxylic acid groups [14, 21, 23], as well as 11-aminoundecanoic acid and subsequently a fluorescent dye (Alexa Fluor 488 or fluorescein-5-isothiocyanate (FITC)) [14]. Single-segment gold nanowires have been functionalized with thiols including the thioacetate-terminated thiol P-SAc [24] and 1,9-nonanedithiol with the fluorescent dye Alexa Fluor 546 [14].

Multisegment nanowires are attractive because the differences in surface chemistry between different segments makes possible spatially resolved chemical functionalization with multiple molecules on the same nanowire, with different ligands directed to different segments. Our work with two-segment Ni–Au nanowires serves as an example of this spatially resolved functionalization. In one scheme, after exposure to HemIX, Ni–Au nanowires showed strong fluorescence from the Ni segments, and the Au segment exhibited weak fluorescence due to nonspecific HemIX adsorption. However, after simultaneous functionalization with HemIX and Au-specific nonylmercaptan, only the Ni segments showed fluorescence, indicating that the nonylmercaptan had attached to the Au segment to prevent nonspecific binding of HemIX [14,24]. Bauer and co-workers also reacted Ni–Au nanowires with 11-aminoundecanoic acid and nonylmercaptan, and then subsequently with Alexa Fluor 488, which binds only to the 11-aminoundecanoic acid. Selective functionalization caused only the Ni segment to fluoresce, as shown in Figures 1.8a and 1.8b. Conversely, reacting the Ni–Au wires with 1,9-nonanedithiol and palmitic acid (for specific binding to Ni), and then with Alexa Fluor 546, which binds only to the 1,9-nonanedithiol, resulted in fluorescence of only the Au segment. Lastly, exposing Ni–Au nanowires to both 11-aminoundecanoic acid and 1,9-nonanedithiol, and then adding the fluorescent markers Alexa Fluor 488 and 546, resulted in fluorescence of both segments.

Selective surface functionalization of nanowires has also been accomplished with biomolecules. In one study, single-segment nickel and gold nanowires were functionalized with palmitic acid and an ethylene glycol-terminated alkanethiol, respectively, to render the nickel hydrophobic and the gold hydrophilic. Two-segment Ni–Au nanowires were exposed to both reagents. The nanowires were then exposed to Alexa Fluor 594 goat anti-mouse IgG protein, an antibody with an attached fluorescent tag. It is known that proteins are able to attach noncovalently to hydrophobic surfaces, but are prevented from such binding to hydrophilic surfaces. As seen in Figures 1.8c and 1.8d, only the nickel surfaces showed fluorescence, confirming that they had been selectively functionalized with the protein [31].

Other experiments involving functionalization with biomolecules have used two-segment Ni–Au nanowires as synthetic gene-delivery systems [32]. DNA plasmids encoding fluorescent proteins were bound to the nickel segment through a carboxylic acid intermediary, while the cell-targeting protein transferrin was bound to the gold segment through a thiolate linkage. This application of biomolecule-functionalized nanowires to gene delivery is detailed in Section 1.9.

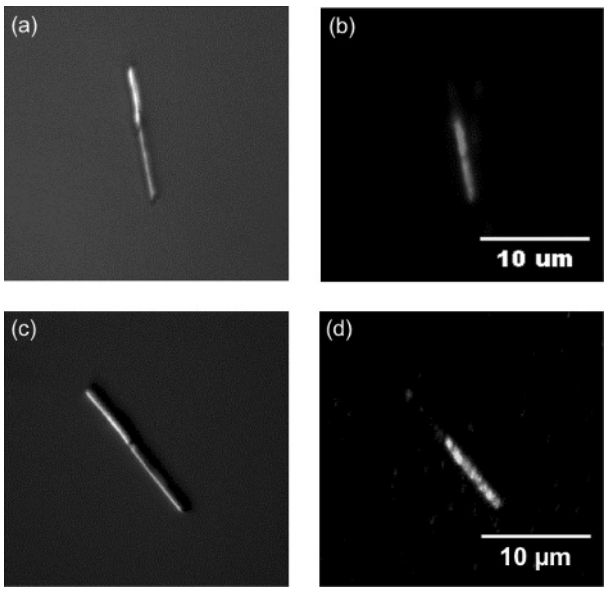

Figure 1.8. (a, b) Two-segment Ni-Au nanowire, functionalized with 11-aminoundecanoic acid and nonylmercaptan, and reacted with Alexa Fluor 488. (Reprinted with permission from Ref. 14. Copyright 2003 American Chemical Society.) (a) Reflected light image. (b) Fluorescent image showing fluorescence from Ni segment only. (c, d) Two-segment Ni–Au nanowire functionalized with palmitic acid and an ethylene glycol-terminated alkanethiol followed by exposure to a fluorescent protein. (c) Reflected light image, (d) Fluorescence image of Ni segment. (Reprinted with permission from Ref. 31. Copyright 2003 American Chemical Society.)

1.6 RECEPTOR-MEDIATED SELF-ASSEMBLY OF NANOWIRES

Chemical functionalization has also been used as a means to position nanowires using receptor-mediated binding to tether nanowires to specific regions of a substrate. This technique again has many potential biological applications, ranging from cell positioning to biosensing. Salem et al. [33] have demonstrated this technique using two-segment Ni–Au nanowires, with 8 μm Ni segments and 1 μm Au segments. These nanowires were functionalized by exposure to a solution of palmitic acid and thiol-terminated biotin. The biotin bound preferentially to the gold segment, and the palmitic acid coated the nickel segment to prevent nonspecific binding of the biotin to the remainder of the nanowire. Stripes of avidin were patterned via microfluidics on a silver film that was first coated with thiol-terminated biotin. Upon introduction of the biotinylated nanowires, the gold ends of the nanowires were anchored to the patterned regions of the substrate by the strong linkage between avidin and biotin, resulting in directed assembly of nanowires in the striped regions, as shown in Figure 1.9. These robust and flexible linkages allowed the nanowires to be pivoted about their binding points to align with an external magnetic field.

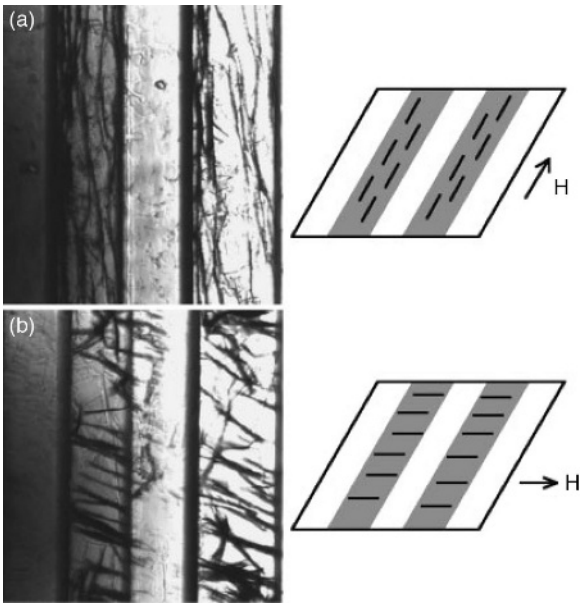

Figure 1.9. Optical images and schematic illustrations of receptor-mediated nanowire self-assembly. Chemically functionalized Ni–Au nanowires are selectively anchored by their gold ends to patterned stripes of avidin on the substrate. A magnetic field is applied parallel (A) and perpendicular (B) to the stripes, resulting in pivoting about the nanowire binding points. (Reprinted with permission from Ref. 33.)

1.7 MAGNETIC SENSING OF NANOWIRES

Detection and identification of biomolecules is becoming a crucial component of many biotechnological applications, and magnetic biosensing is a rapidly developing and evolving field [9,10,34–38]. The typical approach to magnetic biosensing uses integrated arrays of magnetic field sensors, such as GMR devices or magnetic tunnel junctions [35,36], whose surfaces are functionalized with receptor ligands for analytes of interest. If an analyte is labeled with a magnetic nanoparticle, its presence can then be detected by the action of the nanoparticle's magnetic field on the sensor when the analyte binds to the surface of the sensor. This thus provides an alternative approach to commonly used immunofluorescence-based detection techniques, such as ELISA.

Nanowires have shown potential for use in biosensing applications. Many of the magnetic biosensing schemes currently in development use superparamagnetic beads as the tagging particles, which requires the use of an external magnetic field to magnetize the beads. However, due to their large remanent moment, magnetic detection of nanowires can be performed in the absence of a large external magnetic field. We have demonstrated the feasibility of detection of ferromagnetic nanowires, as shown in Figure 1.10. Using GMR sensors as detectors [39], we find that both the presence and orientation of single wires are readily detectable, which may make possible a number of

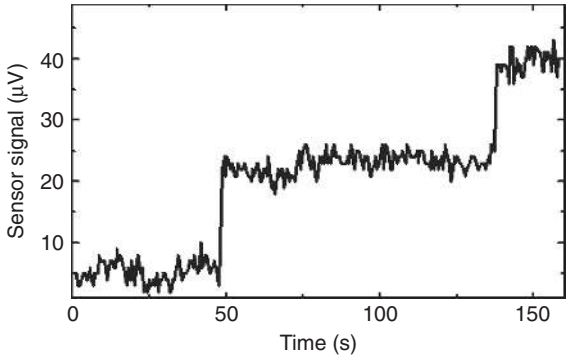

Figure 1.10. Voltage versus time trace for two 5 μm nanowires detected by a GMR sensor. (Reprinted with permission from Ref. 39 © 2004 IEEE.)

biological applications of GMR devices that complement the coverage assays currently implemented with beads.

1.8 APPLICATION OF FORCE TO CELLS

The tunable magnetic and chemical properties of nanowires make them an excellent vehicle for applying forces to cells. Superparamagnetic beads have been in use for some time as means of force application in biological systems [1–8], but are generally available only in a spherical geometry and with a single surface chemistry. Nanowires, however, offer several advantages through the tunability of their magnetic properties. Ferromagnetic nickel nanowires, for example, feature a large remanent magnetization; therefore, they can apply large forces in small magnetic fields, as well as a saturation magnetization that allows for large forces in increased magnetic fields. Furthermore, the nanowires' dimensions can be adjusted to span relevant biological length scales. As we will show, this latter property offers additional versatility in controlling cell–nanowire interactions.

The binding and internalization of nanowires by cells was investigated by immunofluorescent staining of NIH 3T3 mouse fibroblast cells with attached nanowires for the focal adhesion protein paxillin [40]. The results indicate the presence of focal adhesions containing paxillin along the length of the nanowires on short timescales, as seen in Figures 1.11A and 1.11B. The focal adhesions disappear within several hours, suggesting that the nanowires have been internalized inside the cell membrane. This was confirmed by coating nanowires with mouse IgG protein and then incubating them with cells for different durations. After short incubation times, exposure to Alexa Fluor 488 conjugated goat anti-mouse IgG fluorescently labeled nanowires that were attached to the cell membrane but not internalized (Figures 1.11C and 1.11D), while after longer incubation times nanowires remained unlabeled, indicating that they had been internalized and thus protected from the stain. This indicates that the nanowires that were internalized into the cell through integrin-mediated phagoctytosis.

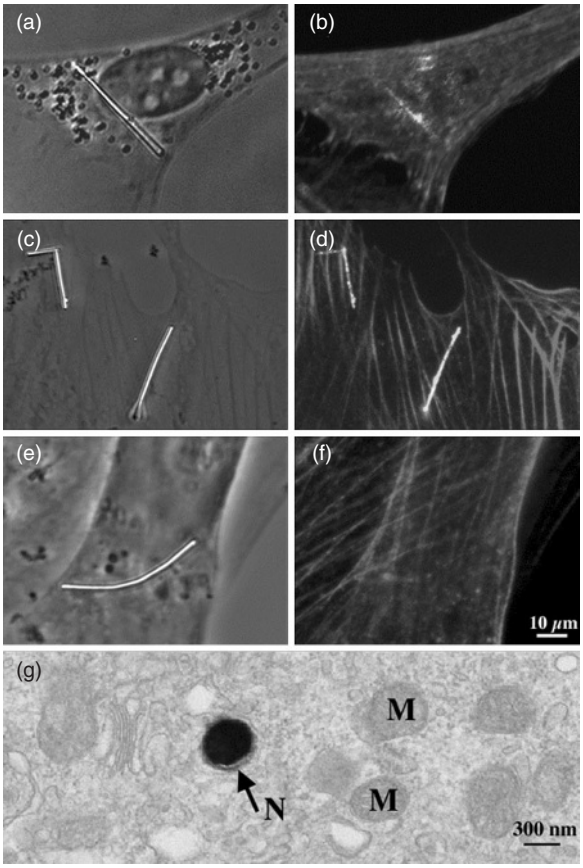

Figure 1.11. Binding of cell to nanowire. Top row: (a) Phase contrast image of a cell incubated with a 35 μm nanowire for 30 min and (b) fluorescence image of the same cell indicating paxillin focal adhesions. Second row: (c) Phase contrast image of a cell after a 30 min incubation with mouse IgG-coated nanowires and (d) fluorescence image of the same cell showing immunofluorescent staining of mouse IgG on the nanowire, indicating that the nanowire is external to the cell. Third row: (e) Phase contrast image of a cell after a 24 hr incubation with mouse IgG-coated nanowires and (f) fluorescense image of the same cell. The mouse IgG on the nanowire is unstained, indicating that the nanowire is internalized. (g) TEM image of a cell incubated with a nanowire for 24 hr. N, nanowire; M, mitochondria. (Reprinted with permission from Ref. 40. Copyright 2005 American Chemical Society.)

Attaching magnetic nanowires to cells has enabled their use as a tool for performing magnetic cell separations. In this process, magnetic particles are bound to cells in a mixture, which is then put in suspension in a magnetic field gradient. The field gradient creates a force that collects only cells with attached magnetic particles. Due to their higher magnetic moment, nickel nanowires have been shown to outperform superparamagnetic beads when separating cells with attached magnetic particles from

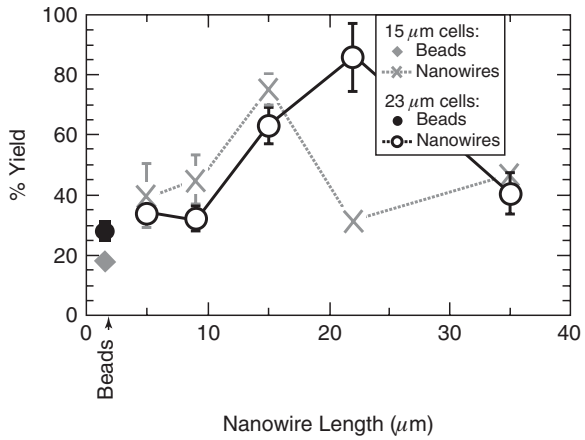

Figure 1.12. Percent yield versus nanowire length for separations using 15 and 23 μm-diameter cells. Data for superparamagnetic beads provided for reference. (Reprinted with permission from Ref. 40. Copyright 2005 American Chemical Society.)

those without [13,40]. Further studies have demonstrated that separations with nanowires become more effective as the length of the nanowires is increased, and they are optimized when the nanowire length matches the diameter of the cell [17]. This has been confirmed with 3T3 cells whose average size was increased by exposure to the cell division inhibitor mitomycin-C. Figure 1.12 shows that the maximum in the separation yield versus nanowire length tracks the increase in cell diameter.

The manner in which nanowires of different lengths interact with cells was explored to account for this finding. For nanowires with lengths less than the cell diameter, internalized nanowires are entirely inside the cell membrane when the cell is in suspension, as is the case in Figures 1.13A and 1.13B. However, nanowires with lengths greater than the cell diameter cannot be enclosed by the suspended cells, as seen in Figures 1.13C–E. It is likely that mechanical forces on the nanowire ends protruding from the cell membrane of suspended cells cause these nanowires to detach from the cells in some cases, accounting for the reduction in cell separation yield encountered when the nanowire length exceeds the suspended cell's diameter [40].

This dependence on nanowire length in nanowire–cell interactions may provide a new way to select among cells in a heterogeneous population. For example, cell separations have been performed with cell mixtures, in which half of the cells have had their diameter increased through exposure to mitomycin-C. Nanowires with lengths matched to the cells of smaller diameter separated cells of both diameters in equal proportions, while nanowires matched to the cells of larger diameter separated a higher proportion of larger cells [40]. This result suggests that it is possible to use magnetic nanowires to separate heterogeneous cell mixtures based on differences in the physical size of the cells.

Magnetic nanowires attached to cells can also be used to assemble multicellular constructs and microarrays of cells. We have used nanowires to direct the self-assembly

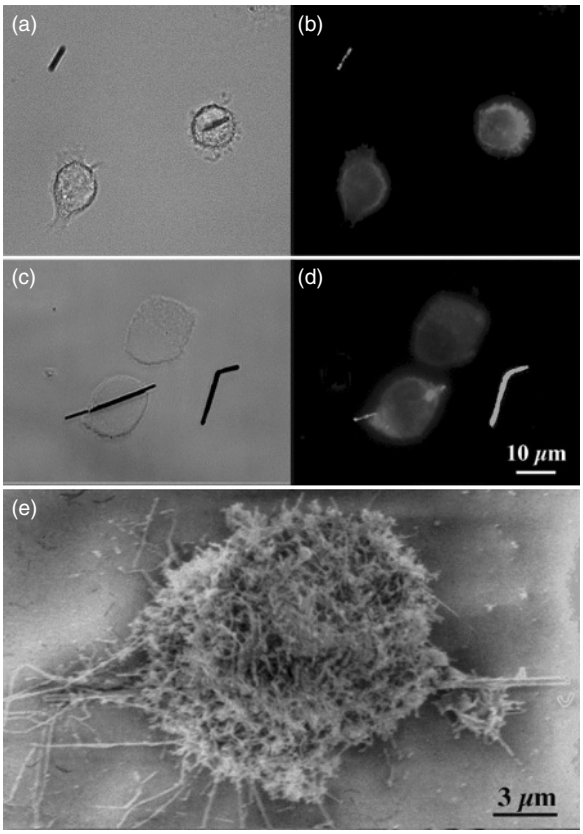

Figure 1.13. Optical images of suspended 3T3 cells. Top row: Suspended cell bound to a 9 μm mouse IgG coated nanowire. (a) Transmitted light and (b) composite fluorescense image of the same cell showing actin filaments and staining of the mouse IgG on an isolated nanowire (upper left) but not of the bound nanowire that is in the cell. Second row: Suspended cell bound to a 22 μm mouse IgG-coated nanowire. (c) Transmitted light and (d) composite fluorescent image of the same cell showing actin filaments and staining of the mouse IgG on both the portion of the nanowire that is no lkonger internal to the cell and on the isolated nanowire (right). (e) SEM image of a cell bound to a 22 μm nanowire. (Reprinted with permission from Ref. 40. Copyright 2005 American Chemical Society.)

of one-dimensional chains of cells by placing suspended cells with attached nanowires in a uniform magnetic field [25]. The chaining process is similar to the one previously described in Section 1.4, the difference being that the viscous drag due to the attached cells is significantly larger than that of just the nanowires, resulting in reduced motion during the chaining. Figure 1.14 illustrates the cell chaining process with a schematic, and shows images of chained 3T3 cells.

Magnetic manipulation has also been demonstrated as a technique for organizing cells into two-dimensional microarrays [25]. These experiments utilized elliptically

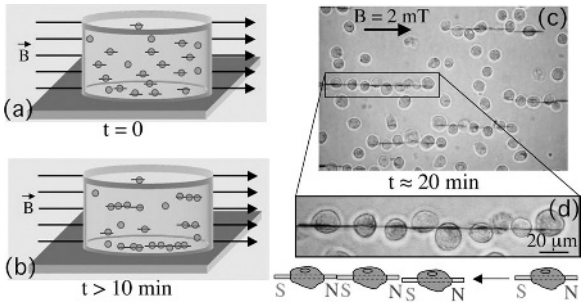

Figure 1.14. Magnetic cell chaining. (a) Schematic of nanowires bound to suspended cells and aligned in a magnetic field B. (b) Schematic of chain formation process due to magnetic dipole–dipole interactions between prealigned nanowires. (c) Cell chains formed on the bottom of a culture dish with $B = 2$ mT. (d) Close-up of a single-cell chain detailing wire–wire alignment. Interactions of North and South poles of adjacent nanowires are indicated schematically below. (From Ref. 25. Reprinted with permission of The Royal Society of Chemistry.)

shaped permalloy micromagnets that were patterned on substrates. A uniform external magnetic field applied parallel to the long axis of the micromagnets magnetized them, and it also co-aligned nanowires with attached cells in suspension in the same direction. The local magnetic field of the micromagnets attracted nearby nanowires to their poles, where their field was most intense, while repelling them from the area above them. An example of cells trapped on the ends of micromagnets in this way is seen in Figure 1.15, along with a graphical representation of the nanowire–micromagnet interaction energy that indicates the repulsive region above the micromagnet and the deep, attractive "wells" at each end.

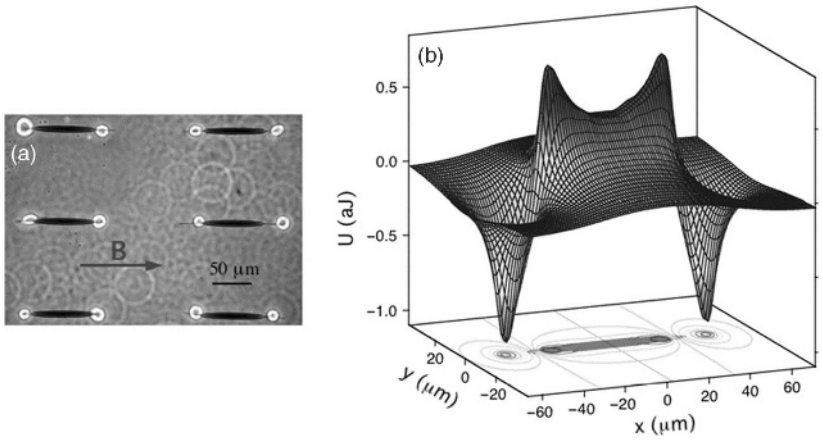

Figure 1.15. (a) Trapping of single cells by ellipsiodal micromagnets. Aligning field $B = 2$ mT. (b) Calculated wire–ellipse interaction energy U_1 at a wire height $z = 3$ μm. Ellipse footprint is shown on the floor of the figure. (From Ref. 25. Reprinted with permission of The Royal Society of Chemistry.)

Patterning hundreds or thousands of micromagnets into rectangular arrays enabled ordered cell trapping in two dimensions, and variation of the spacing between magnets allowed additional control over the type of cell patterns created. As described above, each micromagnet created an attractive region on its ends and a repulsive region above. For isolated micromagnets, as in Figures 1.16a and 1.16d, this resulted in individual points of attraction, whose interaction energy is seen in Figure 1.16g. Micromagnets with their long axes close together exhibited a row of such points that merge together to become

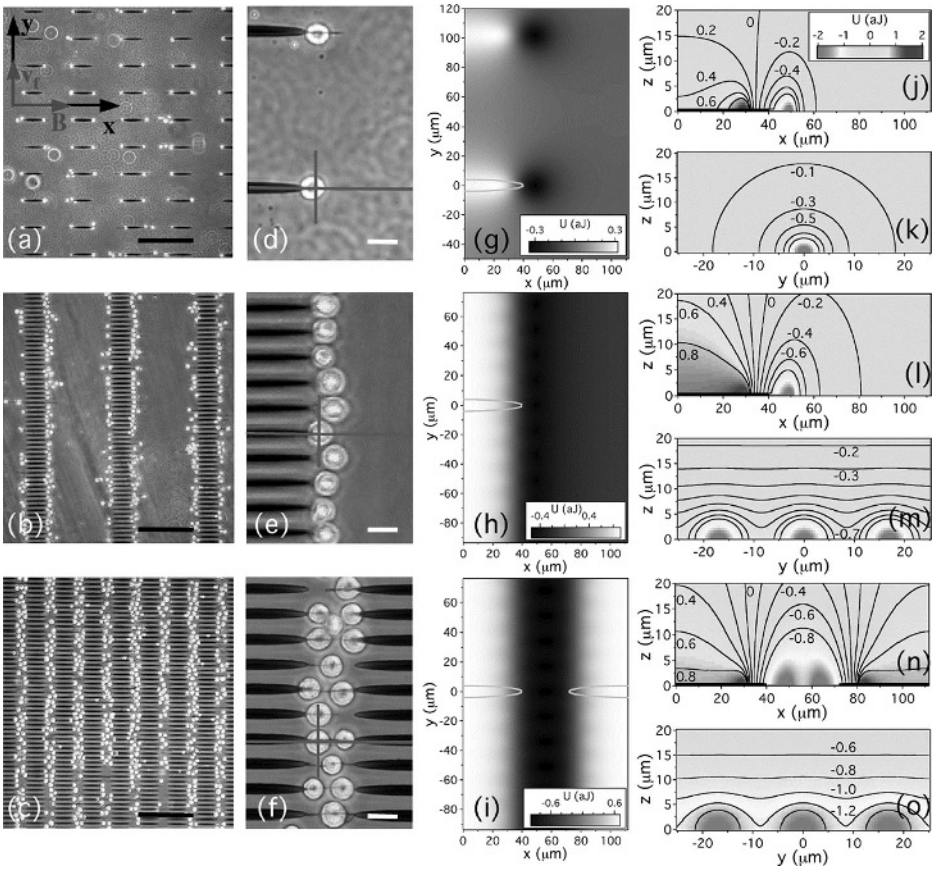

Figure 1.16. (a–c) Overview images of cell trapping on magnetic arrays. The direction of the external field $B = 10$ mT and the fluid flow $Q_f = 1.7\ \mu L\,sec^{-1}$ are shown in (a). The array lattice parameters are (a) $a = 125\ \mu m$, $b = 100\ \mu m$; (b) $a = 260\ \mu m$, $b = 17\ \mu m$; (c) $a = 32\ \mu m$, $b = 17\ \mu m$. Scale bars in (a–c) $= 200\ \mu m$. (d–f) Close-up images of panels (a–c). Scale bars in (d–f) $= 20\ \mu m$. (g–i) Calculated magnetic energy for a cell with a wire at a height $z = 8\ \mu m$ above the regions shown in (d–f). The wire is attracted to dark regions and repelled from white regions. Selected micromagnets are outlined. (j–o) Calculated magnetic energy of wire and cell in vertical planes above the lines in (d–f). The micromagnets appear as thick black lines at the bottom of (j), (l), and (n). (From Ref. 25. Reprinted with permission of The Royal Society of Chemistry.)

an attractive "trough," trapping cells into lines as seen in Figures 1.16b, 1.16e, and 1.16h. Patterning the micromagnets close together in both dimensions effectively merged together the troughs of two adjacent columns of micromagnets to create alternating bands of attractive and repulsive regions. The resultant patterned bands of cells are seen in Figures 1.16c, 1.16f, and 1.16i. The micromagnets can thus be used to create a variety of attractive and repulsive regions on a substrate that lead to two-dimensional organization of cells. Such organization has numerous possible applications, including biosensing, diagnostics, and techniques for tissue engineering.

1.9 NANOWIRE-ASSISTED GENE DELIVERY

The use of synthetic systems for delivering genetic material into cells has several advantages over viral delivery, including ease of production and reduced risk of cytotoxicity and immunogenicity [41, 42]. Previously introduced nonviral gene delivery methods, such as liposomes, polymers, and gold particles, are limited in transfection effectiveness due to difficulties controlling their properties. Nanowires chemically functionalized with biomolecules, however, offer degrees of freedom unavailable to these other methods and indeed have been shown to be an effective tool for nonviral gene delivery [32, 43].

Gene transfection experiments were conducted by Salem et al. [33] using two-segment Ni–Au nanowires with diameter 100 nm and length 200 nm (100 nm Ni, 100 nm Au). DNA plasmids encoding firefly luciferase or green fluorescent protein (GFP) were conjugated to 3-[(2-aminoethyl)dithio] propionic acid (AEDP) that was selectively attached to the nickel surfaces via a carboxylic acid terminus. A thiolate linkage was used to attach transferrin to the gold surfaces. Transferrin was chosen as a cell-targeting protein because all metabolic cells take in iron through receptor-mediated endocytosis of the transferrin–iron complex [44], and thus it would increase the probability of nanowire transport through the cell membrane.

In *in vitro* experiments, functionalized nanowires were incubated with human embryonic kidney cells (HEK293) and were found to be internalized by the cells, as shown by SEM, TEM, and confocal microscopy. Additionally, the cells exhibited fluorescence due to the firefly luciferase or GFP, indicating genetic transfection (Figure 1.17). Nanowires functionalized with both transferrin and DNA plasmid displayed substantially increased luciferase and GFP expression compared to nanowires functionalized only with DNA, confirming that the transferrin was effective in promoting transfection through receptor-mediated endocytosis.

To test the potential utility of multifunctional nanowires for genetic immunization applications, an *in vivo* study was done to measure the immune response in mice to cutaneous delivery via gene gun bombardment of nanowires functionalized with the model antigen ovalbumin and a DNA plasmid that further stimulates the immune response [43]. Both a strong antibody response in the bloodstream and a strong CD8+ T-cell response in the spleen were observed. A comparison of the antibody response for the nanowires with that obtained using 1.6 μm gold particles as the carriers is shown in Figure 1.18. These gold particles are the state of the art in inorganic carriers

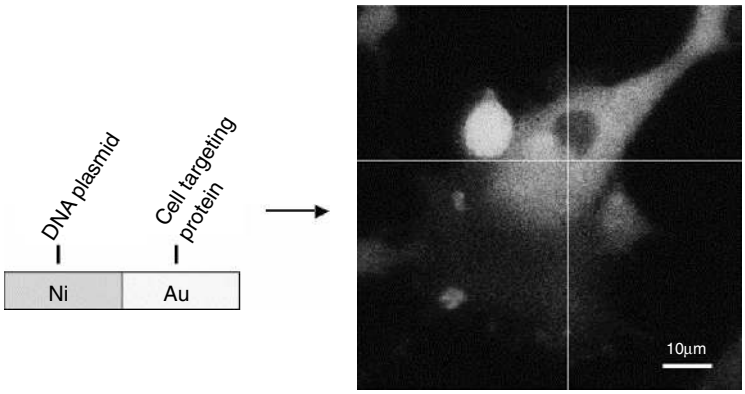

Figure 1.17. Drug delivery using multisegment nanowires, showing HEK cell expressing GFP after transfection by two-segment nanowires carrying GFP plasmid, and the cell-targeting agent transferring. (Reprinted by permission from Macmillan Publishers Ltd, *Nature Materials* [32], copyright 2003.)

for gene gun bombardment, and delivery methods using them have been optimized over a number of years. It is thus quite encouraging that the nanowires generate comparable antibody responses in these initial experiments. In the CD8+ T-cell studies, DNA bound to the nanowires alone generated very low or no response. However, nanowires with both DNA and the ovalbumin produced an eightfold increase in the CD8+ response compared to nanowires carrying only the ovalbumin. These results suggest

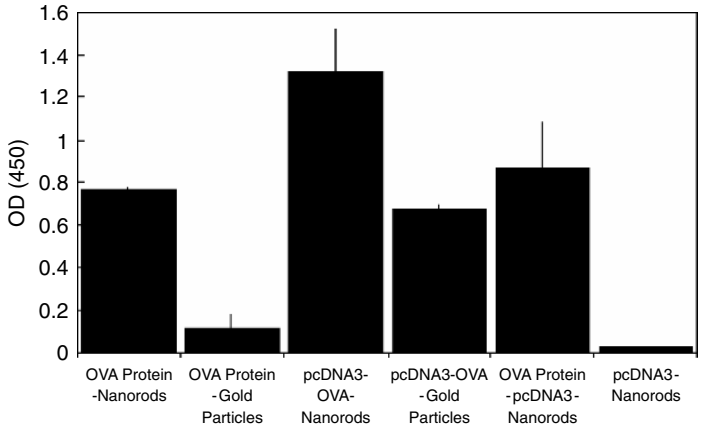

Figure 1.18. Ovalbumin-specific antibody responses in C57BL/6 mice immunized with functionalized Ni–Au nanowires gold particles: Nanowire formulations included ovalbumin protein only (OVA Protein), DNA plasmid encoding ovalbumin only (pcDNA3-OVA), ovalbumin protein and control plasmid (not encoding ovalbumin) (OVA Protein–pcDNA3), and control plasmid only (pcDNA3). Gold particle formulations included ovalbumin protein (OVA Protein) and DNA plasmid encoding ovalbumin protein (pcDNA3-OVA). (Reprinted with permission from Ref. 43.)

that with further optimization, the ability of the nanowires to deliver multiple immunostimulants to the same cell in controlled doses may prove highly effective for genetic immunization.

1.10 SUMMARY

This chapter has presented an overview of recent work on the development and applications of multifunctional magnetic nanowires for biotechnology, including areas such as cell separations, cell positioning and manipulation, and intracellular drug and gene delivery. A wide range of other applications are envisioned or under development, in areas such as tissue engineering, biomagnetic control of cellular function, and subcellular force transduction. It is also important to note that the concept of asymmetric magnetic nanoparticles with spatially resolved chemical functionality need not be limited to electrodeposited nanowires; many other architectures are possible, and indeed some are already under exploration [45]. Thus it seems likely that there will be continued innovation and development of new applications of multifunctional magnetic nanoparticles in biotechnology in the foreseeable future.

REFERENCES

1. Safarik I, Safarikova M. Use of magnetic techniques for the isolation of cells. *J Chromatogr B* 1999;722:33–53.
2. Häfeli U, Schütt W, Teller J, Zborowski M, editors. *Scientific and Clinical Applications of Magnetic Microspheres*. New York: Plenum Press; 1997.
3. MacKintosh FC, Schmidt CF. Microrheology. *Curr Opin Coll Interface Sci* 1999;4:300–307; and references cited therein.
4. Bausch AR, Hellerer U, Essler M, Aepfelbacher M, Sackmann E. Rapid stiffening of integrin receptor-actin linkages in endothelial cells stimulated with thrombin: A magnetic bead microrheology study. *Biophys J* 2001;80:2649–2657.
5. Matthews BD, Overby DR, Alenghat FJ, Karavitis J, Numaguchi Y, Allen PG, Ingber DE. Mechanical properties of individual focal adhesions probed with a magnetic microneedle. *Biochem Biophys Res Commun* 2004;313:758–764.
6. Fabry B, Maksym GN, Butler JP, Glogauer M, Navajas D, Fredberg JJ. Scaling the microrheology of living cells. *Phys Rev Lett* 2001;87:148102.
7. Wang N, Butler JP, Ingber DE. Mechanotransduction across the cell surface and through the cytoskeleton. *Science* 1993;260:1124–1127.
8. Meyer CJ, Alenghat FJ, Rim P, Fong JH, Fabry B, Ingber DE. Mechanical control of cyclic AMP signalling and gene transcription through integrins. *Nat Cell Biol* 2000;2:666–668.
9. Baselt DR, Lee GL, Natesan M, Metzger SW, Sheehan PE, Colton RJ. A biosensor based on magnetoresistance technology. *Biosens Bioelectron* 1998;13:731–739.
10. Li GX, Wang SX, Sun SH. Model and experiment of detecting multiple magnetic nanoparticles as biomolecular labels by spin valve sensors. *IEEE Trans Magn* 2004;40:3000–3002.

11. Pellegrino T, Kudera S, Liedl T, Javier AM, Manna L, Parak WJ. On the development of colloidal nanoparticles towards multifunctional structures and their possible use for biological applications. *Small* 2005;1:48–63; and references therein.
12. Fert A, Piraux L. Magnetic nanowires. *J Magn Magn Mater* 1999;200:338–358; and references therein.
13. Hultgren A, Tanase M, Chen CS, Meyer GJ, Reich DH. Cell manipulation using magnetic nanowires. *J Appl Phys* 2003;93:7554–7556.
14. Bauer LA, Reich DH, Meyer GJ. Selective functionalization of two-component magnetic nanowires. *Langmuir* 2003;19:7043–7048.
15. Chen M, Sun L, Bonevitch JE, Reich DH, Chien CL, Searson PC. Tuning the response of magnetic suspensions. *Appl Phys Lett* 2003;82:3310–3312.
16. Ji C, Searson PC. Synthesis and characterization of nanoporous gold nanowires. *J Phys Chem B* 2003;107:4494–4499.
17. Hultgren A, Tanase M, Chen CS, Reich DH. High-yield cell separations using magnetic nanowires. *IEEE Trans Magn* 2004;40:2988–2990.
18. Chen M, Searson PC, Chien CL. Micromagnetic behavior of electrodeposited Ni/Cu nanowires. *J Appl Phys* 2003;93:8253–8255.
19. Chen M, Hao Y, Chien CL, Searson PC. Tuning the properties of magnetic nanowires. *IBM J Res Dev* 2005;49:79–102.
20. Nicewarner-Pena SR, Freeman RG, Reiss BD, He L, Pena DJ, Walton ID, Cromer R, Keating CD, Natan MJ. Submicrometer metallic barcodes. *Science* 2001;294:137–141.
21. Tanase M, Bauer LA, Hultgren A, Silevitch DM, Sun L, Reich DH, Searson PC, Meyer GJ. Magnetic alignment of fluorescent nanowires. *Nano Lett* 2001;1:155–158.
22. Tanase M, Silevitch DM, Hultgren A, Bauer LA, Searson PC, Meyer GJ, Reich DH. Magnetic trapping and self-assembly of multicomponent nanowires. *J Appl Phys* 2002;91:8549–8551.
23. Chien CL, Sun L, Tanase M, Bauer LA, Hulgren A, Silevitch DM, Meyer GJ, Searson PC, Reich DH. Electrodeposited magnetic nanowires: Arrays, field-induced assembly, and surface functionalization. *J Magn Magn Mater* 2002;249:146–155.
24. Reich DH, Bauer LA, Tanase M, Hultgren A, Chen CS, Meyer GJ. Biological applications of multifunctional magnetic nanowires (invited). *J Appl Phys* 2003;93:7275.
25. Tanase M, Felton EJ, Gray DS, Hultgren A, Chen CS, Reich DH. Assembly of multicellular constructs and microarrays of cells using magnetic nanowires. *Lab Chip* 2005;5:598–605.
26. Roberts C, Chen CS, Mrksich M, Martichonok V, Ingber DE, Whitesides GM. Using mixed self-assembled monolayers presenting RGD and (EG)3OH groups to characterize long-term attachment of bovine capillary endothelial cells to surfaces. *J Am Chem Soc* 1998;120:6548–6555.
27. Baker M, Jennings G, Laibinis P. Underpotentially deposited copper promotes self-assembly of alkanephosphonate monolayers on gold substrates. *Langmuir* 2000;16:3288–3293.
28. Folkers J, Gorman C, Laibinis P, Buchholz S, Whitesides G. Self-assembled monolayers of long-chain hydroxamic acids on the native oxides of metals. *Langmuir* 1995;11:813–824.
29. Martin CR. Nanomaterials: A membrane-based synthetic approach. *Science* 1994;266:1961–1966.
30. Penner RM, Martin CR. Preparation and electrochemical characterization of ultramicroelectrode ensembles. *Anal Chem* 1987;59:2625–2630.

31. Birenbaum NS, Lai BT, Chen CS, Reich DH, Meyer GJ. Selective noncovalent adsorption of protein to bifunctionalized metallic nanowire surfaces. *Langmuir* 2003;19:9580–9582.
32. Salem AK, Searson PC, Leong KW. Multifunctional nanorods for gene delivery. *Nat Mater* 2003;2:668–671.
33. Salem AK, Chao J, Leong KW, Searson PC. Receptor mediated self-assembly of multi-component magnetic nanowires. *Adv Mater* 2004;16:268–271.
34. Reiss G, Brueckl H, Huetten A, Schotter J, Brzeska M, Panhorst M, Sudfield D, Becker A, Kamp PB, Puehler A, Wojczykowski K, Jutzi P. Magnetoresistive sensors and magnetic nanoparticles for biotechnology. *J Mater Res* 2005;20:3294–3302.
35. Shen WF, Liu XY, Mazumdar D, Xiao G. *In situ* detection of single micron-sized magnetic beads using magnetic tunnel junction sensors. *Appl Phys Lett* 2005;86:253901.
36. Tondra M, Popple A, Jander A, Millen RL, Pekas N, Porter MD. Microfabricated tools for manipulation and analysis of magnetic microcarriers. *J Mang Mater* 2005;293:725–730.
37. Wang SX, Bae SY, Li GX, Sun SH, White RL, Kemp JT, Webb CD. Towards a magnetic microarray for sensitive diagnositics. *J Mang Magn Mater* 2005;293:731–736.
38. Graham DL, Ferreira HA, Feliciano N, Freitas PP, Clarke LA, Amaral MD. Magnetic field-assisted DNA hybridisation and simultaneous detection using micron-sized spin-valve sensors and magnetic nanoparticles. *Sens Actuators B Chem* 2005;107:936–944.
39. Anguelouch A, Reich DH, Chien CL, Tondra M. Detection of magnetic nanowires using GMR sensors. *IEEE Trans Mag* 2004;40:2997–2999.
40. Hultgren A, Tanase M, Felton EJ, Bhadriraju K, Salem AK, Chen CS, Reich DH. Optimization of yield in magnetic cell separations using magnetic nanowires of different lengths. *Biotechol Prog* 2005;21:509–515.
41. Carter PJ, Samulski RJ. Adeno-associated viral vectors as gene delivery vehicles (review). *Int J Mol Med* 2000;6:17–27.
42. Pouton CW, Seymour LW. Key issues in non-viral gene delivery. *Adv Drug Deliv Rev* 2001;46:187–203.
43. Salem AK, Hung CF, Kim TW, Wu TC, Searson PC, Leong KW. Multi-component nanorods for vaccination applications. *Nanotechnology* 2005;16(4):484–487.
44. Wagner E, Curiel D, Cotten M. Delivery of drugs, proteins and genes into cells using transferrin as a ligand for receptor-mediated endocytosis. *Adv Drug Deliv Rev* 1994;14:113–135.
45. Yu H, Chen M, Rice PM, Wang SX, White RL, Sun SH. Dumbbell-like bifunctional Au–Fe3O4 nanoparticles. *Nano Lett* 2005;5m379–382.